Boletín Geológico

SERVICIO GEOLÓGICO COLOMBIANO

Boletín Geológico, 47, 85-105, 2020
https://doi.org/10.32685/0120-1425/boletingeo.47.2020.527

Received: June 1, 2020
Revised: September 24, 2020
Accepted: October 23, 2020
Published online: December 28, 2020

Review of geothermochronological and thermobarometric techniques for the construction of cooling and exhumation curves or paths for intrusive igneous rocks

Revisión de técnicas geotermocronológicas y termobarométricas para la construcción de curvas o trayectorias de enfriamiento y exhumación en rocas ígneas intrusivas

Lina María **Cetina**[1], Julián Andrés **López-Isaza**[1], Mario Andrés **Cuéllar-Cárdenas**[1], Anny Julieth **Forero-Ortega**[1]

1. Dirección Técnica de Geociencias Básicas, Servicio Geológico Colombiano (SGC), Bogotá, Colombia.
Corresponding autor: Lina María Cetina, lcetina@sgc.gov.co

Abstract

The present study reviews radiometric and thermobarometric techniques used to construct cooling curves or paths to characterize intrusive bodies and to calculate cooling and exhumation rates. To construct these curves or paths, the temperature, time and depth variables must be estimated in intrusive bodies by applying various analytical techniques, including thermobarometry and U-Pb zircon, Ar-Ar hornblende and muscovite, fission track and (U-Th)/He zircon and apatite dating, in combination with a geological framework of reference for each intrusive body. The authors recommend to determine the crystallization age by zircon U-Pb dating, to quantify the emplacement depth using thermobarometry methods according to the composition of the intrusive body, to calculate the initial cooling ages with hornblende and muscovite Ar-Ar methods, as well as to calculate the cooling/exhumation ages in the upper crust using low-temperature thermochronology methods. These cooling curves or paths in intrusive bodies are highly relevant when studying compressive or extensional areas because they partly represent the thermal history of the era, thereby providing data on the magmatic and tectonic evolution of the region. Thus, these studies are highly important for designing geodynamic models and for their possible application in developing the tectonic model of the country.

Keywords: cooling and exhumation curves or paths, geochronology, thermochronology, thermobarometry in igneous rocks.

Resumen

El presente trabajo expone una revisión de técnicas radiométricas y termobarométricas para construir curvas o trayectorias de enfriamiento aplicadas a la caracterización de intrusivos, así como el cálculo de tasas de enfriamiento y exhumación. Para la construcción de estas curvas o trayectorias se deben estimar en los intrusivos las variables de temperatura, tiempo y profundidad,

Citation: Cetina, L. M., López-Isaza, J. A., Cuéllar-Cárdenas, M. A., & Forero-Ortega, A. J. (2020). Review of geothermochronological and thermobarometric techniques for the construction of cooling and exhumation curves or paths for intrusive igneous rocks. *Boletín Geológico, 47*, 85-105, https://doi.org/10.32685/0120-1425/boletingeo.47.2020.527

aplicando diversas técnicas analíticas que incluyen termobarometría y geotermocronología U-Pb en circón, Ar-Ar en hornblenda y moscovita, y trazas de fisión y (U-Th)/He en circón y apatito, esto integrado a un marco geológico de referencia para cada intrusivo. Se recomienda determinar la edad de cristalización mediante U-Pb en circón, cuantificar la profundidad del emplazamiento utilizando métodos de termobarometría según la composición del intrusivo, calcular edades de enfriamiento inicial con los métodos Ar-Ar en hornblenda y moscovita, y calcular edades de enfriamiento/exhumación en corteza superior mediante métodos de termocronología de baja temperatura. Estas curvas o trayectorias de enfriamiento en intrusivos son de gran relevancia para estudiar áreas compresivas o extensionales, pues representan en parte la historia termal de la zona y, por lo tanto, proporcionan información sobre la evolución magmática y tectónica de la región. Por lo expuesto, estos estudios son de gran importancia para la formulación de modelos geodinámicos y su posible aplicación en la construcción del modelo tectónico del país.

Palabras clave: curvas o trayectorias de enfriamiento y exhumación, geocronología, termocronología, termobarometría en rocas ígneas.

1. Introduction

Cooling processes inside the earth's crust result from geological events, and their characterization makes it possible to learn the thermal history of a region and to obtain information about their magmatic, metamorphic and tectonic evolution (cf. Dodson, 1979; Harrison et al., 1979; Zeitler, 1985; Green, Duddy, Laslett et al., 1989, Corrigan, 1991; Gallagher et al., 1998, Reiners and Brandon, 2006). In recent decades, different radiometric dating techniques have been combined to construct cooling curves or paths in rock bodies (since isotopic systems are essentially a form of geothermometry) in order to understand the dynamics of orogenic belts and sedimentary basins, as well as their relationships with mineral deposits and petroleum systems (cf. Zeitler, 1985; Green, Duddy, Gleadow et al., 1989; Hunziker et al., 1992; Gallagher et al., 1998; McInnes et al., 1999; Armstrong, 2005; Bernet et al., 2006, Peyton and Carrapa, 2013 a, b; Bernet et al., 2019).

In regions with tectonic deformation, applying various radiometric techniques may help to constrain the exhumation time and rates, and if the exhumation results from tectonic activity, these techniques may help to determine the time of the tectonic events occurred (cf. Zeitler et al., 1982; Bernet et al., 2006; Deeken et al., 2006; Peyton and Carrapa, 2013a); however, exhumation processes are also related to erosion and climatic effects, as well as the combination of these processes to a greater extent (cf. Zeitler, 1985; Brandon et al., 1998; England and Molnar, 1990; Ring et al., 1999; Reiners and Brandon, 2006; Peyton and Carrapa, 2013a; Bernet et al., 2019).

Constructing cooling and exhumation curves for intrusive igneous rocks is an excellent opportunity to partly retrace the thermal and tectonic evolution of a region due to its extensive exposure. In addition, determining the formation age of the intrusive body can constrain deformation and post-deformation times, and offer a first-order view of the uplift or subsidence of the crust during tectonic processes (Harrison et al., 1979; Zeitler, 1985; Hurford, 1986; Anderson et al., 1988; Clarke, 1992; Anderson, 1996; Foster et al., 2001; Anderson et al., 2008; Glorie et al., 2017; Nieto Samaniego et al., 2019).

In Colombia, various radiometric techniques have been used in intrusive rocks to determine crystallization and cooling ages (e.g., *Catalogo de dataciones radiometricas de Colombia*, cf. Gomez et al., 2015), as well as cooling and exhumation studies in intrusive bodies using low-temperature thermochronology techniques (e.g., Sáenz et al., 1996; Sáenz, 2003; Restrepo-Moreno et al., 2009; Villagómez et al., 2011; Cardona et al., 2011; Villagómez and Spikings, 2013; Van der Lelij et al., 2016; León et al., 2018; Restrepo-Moreno et al., 2019). In turn, few thermobarometry studies have estimated the emplacement depth of igneous bodies exposed in the country (Martínez and Zuluaga, 2010; Gil-Rodríguez, 2014; Cortés-Calderón, 2015).

Despite the large volume of geothermochronological data on intrusive units published in the literature, few studies have focused on constructing the cooling and exhumation curves or paths of these units for understanding the evolution of areas with magmatic belts. For this purpose, the authors of this review suggest to consider that: a) reported radiometric data should be statistically validated to increase the reliability of crystallization and cooling ages of intrusive units, b) thermobarometry studies should be performed in intrusive rocks to quantify the emplacement levels of these bodies and c) carrying out systematic studies that combine the different techniques used to the construction of cooling curves or paths in intrusive rocks.

The aim of this review is to present a proposal to construct cooling curves or paths for studying the thermal history of intrusive units in Colombia, to perform a literature review on the currently used analytical techniques, and to highlight the importance of these cooling curves or paths as a complementary tool for determining the geological evolution of the respective units through geodynamic concepts. These approaches are useful to systematically calculate cooling and exhumation rates, and these inputs may be applied to complete the tectonic model of the country.

1.1 History of cooling and exhumation of intrusive igneous rocks

The exposure of large intrusive bodies in the continental crust suggests that these types of rocks play a key role in the evolution of the continents. Therefore, knowing their cooling and exhumation histories is crucial for understanding the crustal evolution that continental masses experience during tectonic events (cf. Anderson, 1996; Foster et al., 2001; Anderson et al., 2008; Mutch et al., 2016; Reiners et al., 2017, p. 197).

The history of cooling and exhumation of intrusive igneous bodies (cf. Harrison et al., 1979; Harrison and Clarke, 1979; Hurford, 1986; England and Molnar, 1990; Foster et al., 1992; George, 1993; Caggianelli et al., 2000; Parada et al., 2005; Glorie et al., 2017; Bernet et al., 2019; Nieto-Samaniego et al., 2019) can be determined by constructing cooling curves or paths, thereby assessing the temperature, time and depth variables that characterize the body from its initial emplacement to its final exposure on the surface (Figures 1 and 2).

These cooling curves or paths are based on the fact that mineral phases dated by some isotopic method, show typical closing temperatures. Therefore, cooling ages associated with different temperature ranges can be determined in a sample, and to perform temperature vs. age plots. In addition, by thermal field modeling or by assuming a geothermal gradient in the study area, the temperature-time data can be converted into depth-time to estimate the cooling/exhumation rates that are partly associated with tectonic events (cf. Wagner et al., 1977; Zeitler et al., 1982; Zeitler, 1985; Hunziker et al., 1992; Bernet et al., 2006; Reiners et al., 2017, pp. 105-122).

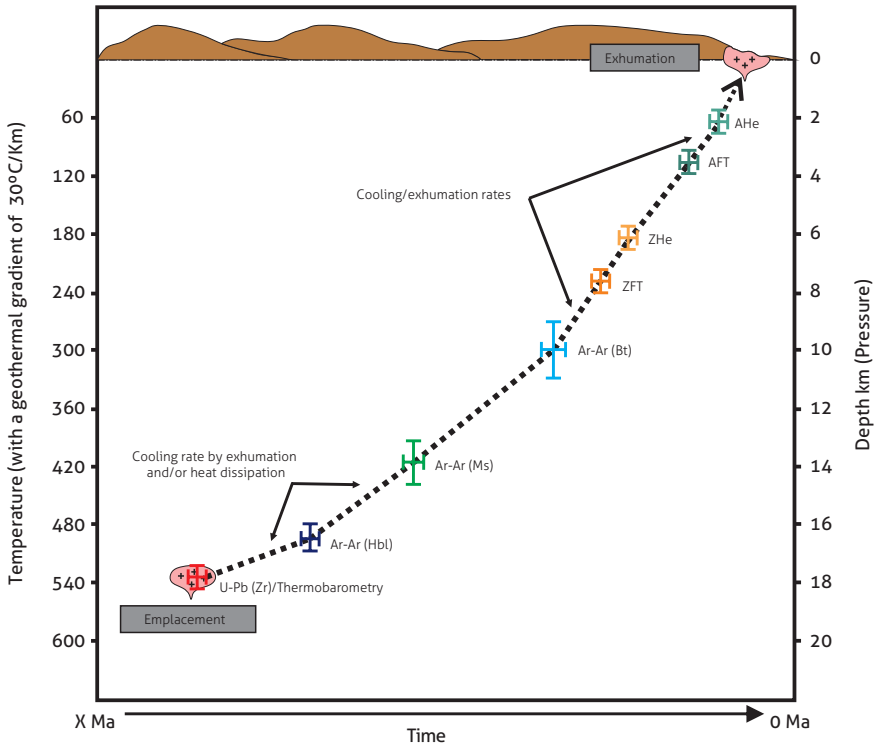

Figure 1. Representative diagram of a hypothetical cooling curve or path of an intrusive body from its emplacement to its final exposure on the surface, indicating the various geothermochronological and thermobarometric methods recommended for determining its cooling/exhumation history. The bars that accompany each method correspond to the uncertainty associated with age and depth. The temperature shown correspond to the hypothetical temperatures of the host rock, according to a geothermal gradient of 30 °C/km. Abbreviations: Zr: zircon; Hbl: hornblende; Ms: muscovite; Bt: biotite; ZFT: fission track in zircon; ZHE: (U-Th)/He in zircon; AFT: fission track in apatite; and AHe: (U-Th)/He in apatite.

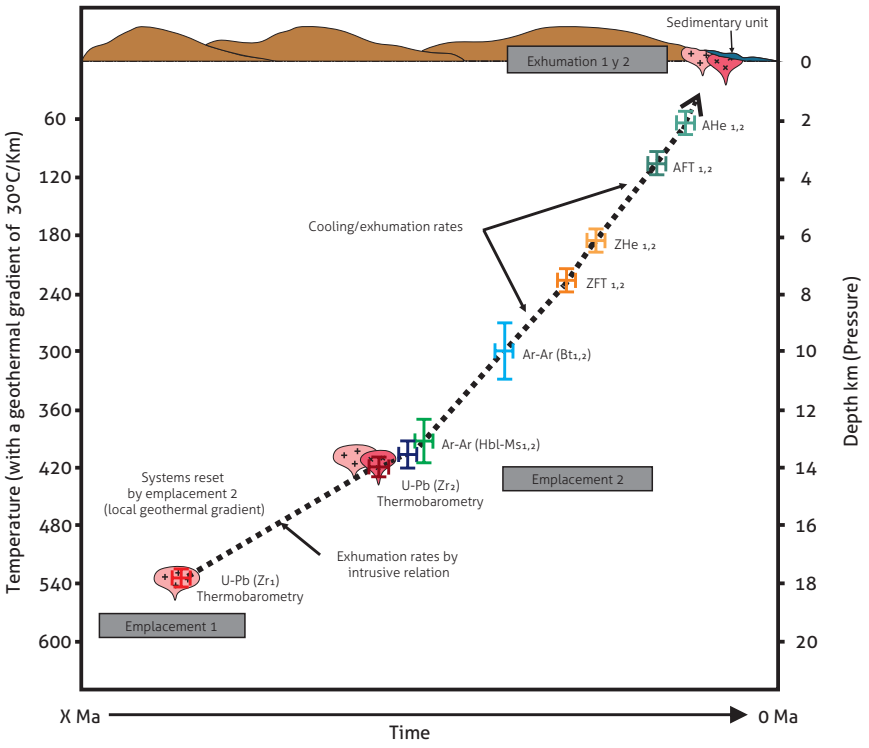

Figure 2. Representative diagram of the cooling curve or path of two intrusive bodies from their emplacement to their final exhumation on the surface showing the field relationships and the geothermochronological and thermobarometric methods recommended for determining their cooling/exhumation history. The bars that accompany each method correspond to the uncertainty associated with age and depth. The temperature shown corresponds to the hypothetical temperature of the host rock according to a geothermal gradient of 30 °C/km. Abbreviations are described in Figure 1.

These cooling curves or paths were initially considered empirically because they represent net histories, which involves simplifying a scenario that may have actually had more complex cooling paths (Zeitler, 1985). However, with sufficient samples and geological data, these curves or paths are highly reliable (Zeitler, 1985) using high-resolution and high-reliability ages and onsidering some type of thermal modeling (cf. Zeitler, 1985; Ehlers, 2005; Ketcham, 2005; Braun et al., 2012).

To properly construct this type of curve or path, the intrusive body should first be geologically characterized, identifying the field relationships with adjacent rocks and the type of contact observed to establish its geological context for reference (Figure 2). This step establishes valid geological criteria that support the interpretation of the findings through various analytical methods. If the unit geological context is clear, cooling and exhumation curves or paths can be constructed by integrating various geothermochronological and thermobarometric methods and by calculating the cooling and exhumation rates of the intrusive body.

2. Proposal for the construction of cooling and exhumation curves or paths of intrusive bodies

The following proposal combines various geothermochronological and thermobarometric methods for determining emplacement (or crystallization) and cooling and/or exhumation ages, according to the closure temperature of each mineral system (Figure 3). These methods also provide key data on the depth associated with each geological process. The application of these analytical methods is conditioned to the nature of the study bodies, that is, they depend on the presence of minerals, such as hornblende, biotite, muscovite, zircon, apatite, and so on. Thus, a sequence of steps is proposed below to gather the necessary data to construct the cooling curves or paths of intrusive rocks:

1. Geological characterization of the intrusive units, determining their nature, geological context and field relationships with adjacent units.

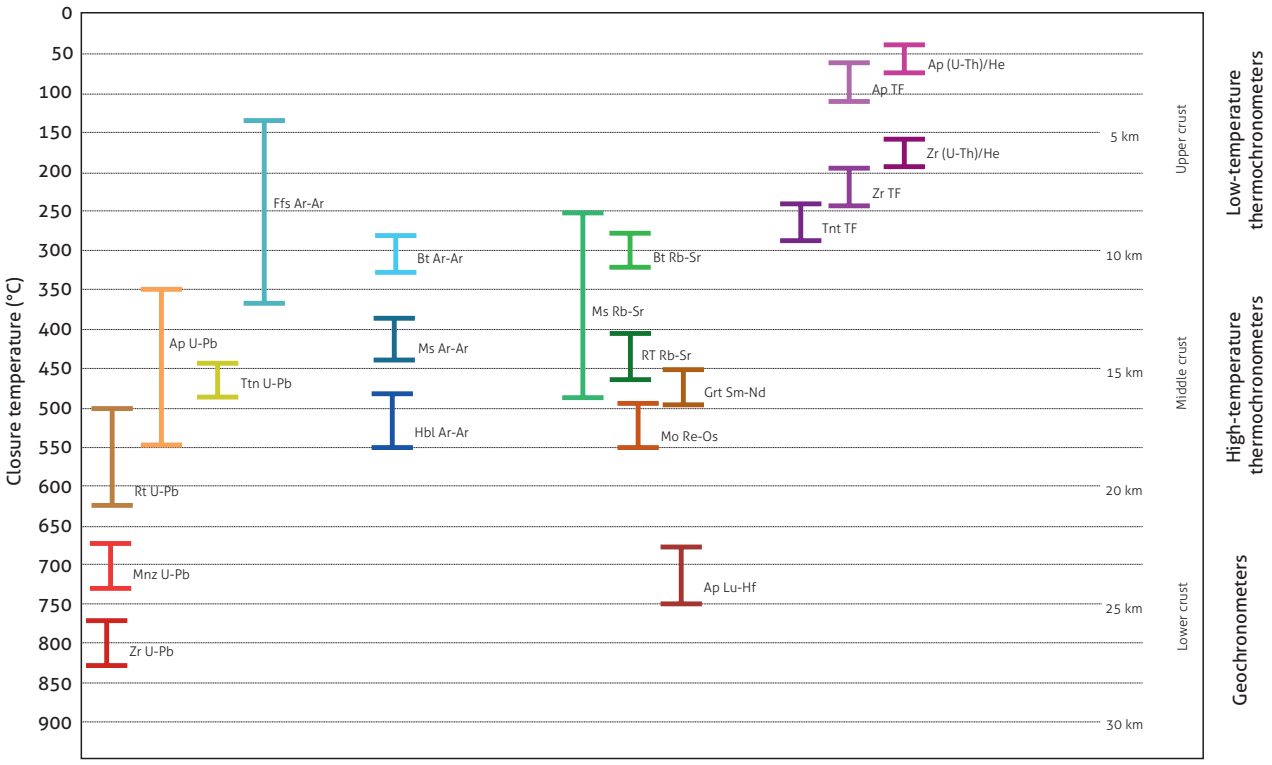

Figure 3. Average closure temperatures of different geothermochronometers and their potential depths, assuming a geothermal gradient of 30 °C/km. Temperature thresholds retrieved from Harrison (1982), Grove and Harrison (1996), Harrison et al., (2009), Chew and Spikings (2015), Bernet et al. (2019) and references therein. Abbreviations: Zr: zircon; Mnz: monazite; Rt: rutile; Ap: apatite; Ttn: titanite; Hbl: hornblende; Ms: muscovite; Bt: biotite; Kfs: potassium feldspar; Mo: molybdenite; Grt: garnet; and FT: fission track.

2. Geological characterization of the units adjacent to the intrusive bodies.
3. Calculation of emplacement (or crystallization) ages using the zircon U-Pb method.
4. Quantitative estimation of emplacement depths using thermobarometry techniques (e.g., aluminum in hornblende barometer), which are also applied to the host rock to estimate the geothermal paleogradient of the emplacement environment.
5. Calculation of initial cooling ages using high-temperature thermochronometers (hornblende and muscovite Ar-Ar).
6. Calculation of cooling ages in the upper crust levels using high-temperature thermochronometers (fission track and zircon and apatite (U-Th)/He dating).
7. Determination of the thermal history of intrusive bodies by combining geothermochronological and thermobarometric data, assuming a geothermal gradient or from thermal field modeling.
8. Calculation of cooling (Δtemperature/Δtime) and exhumation (Δtemperature/geothermal gradient/Δtime) rates.
9. Evaluation of the possible cooling/exhumation mechanisms associated with tectonic events, erosion or both processes.

3. Analytical methods

Obtaining the necessary data to determine the cooling curve or path of intrusive rocks requires applying specific analytical methods, whose particular characteristics will influence the possible interpretations of the results. The methods used to obtain data for constructing the cooling curve or path are described below.

3.1. Zircon U-Pb geochronology: emplacement age

The emplacement age of an intrusive body can be correlated with its crystallization age, which is determined by zircon U-Pb dating (cf. Faure and Messing, 2005; Reiners et al. 2017,

pp. 197-199). Also, the crystallization age of zircon is assumed to be the crystallization age of the igneous body because the mineral has a closure temperature of approximately 900-700 °C (Cherniak and Watson, 2001; Harrison et al., 2007) and an average of 800 °C (Figure 3), at which a melt of intermediate composition would reach 50% crystallization (Carroll and Wyllie, 1990; Harrison et al., 2007).

However, the emplacement of plutonic bodies may involve multiple intrusive facies (cf. Miller et al., 2007; Reiners et al. 2017, pp. 198-199), and due to the crystallization of a zircon mineral depends on zirconium saturation and on the composition and temperature of the melt (Harrison et al., 2007) a granite body may contain zircon xenocrysts, anticrysts and autocrysts, which gives rise to a wide range of zircon U-Pb ages (cf. Coleman et al., 2004; Miller et al., 2007). Xenocrysts are zircons that are foreign to the magmatic melt, which can be derived, for example, from the source rock (in this case, termed inherited zircons) or from the host rock. Anticrysts are zircons formed in the initial magma pulses, and autocrysts are zircons that grow within the main intrusive pulse (Figure 4; Miller et al., 2007).

Based on the above information, the crystallization age of the intrusive body (or emplacement age) corresponds to the population of ages in zircons interpreted as autocrysts, with statistically reliable parameters (cf. Vermeesch, 2018). Thus, to correctly interpret the U-Pb ages in zircon crystals, the following tasks are recommended: a) characterize the mor-

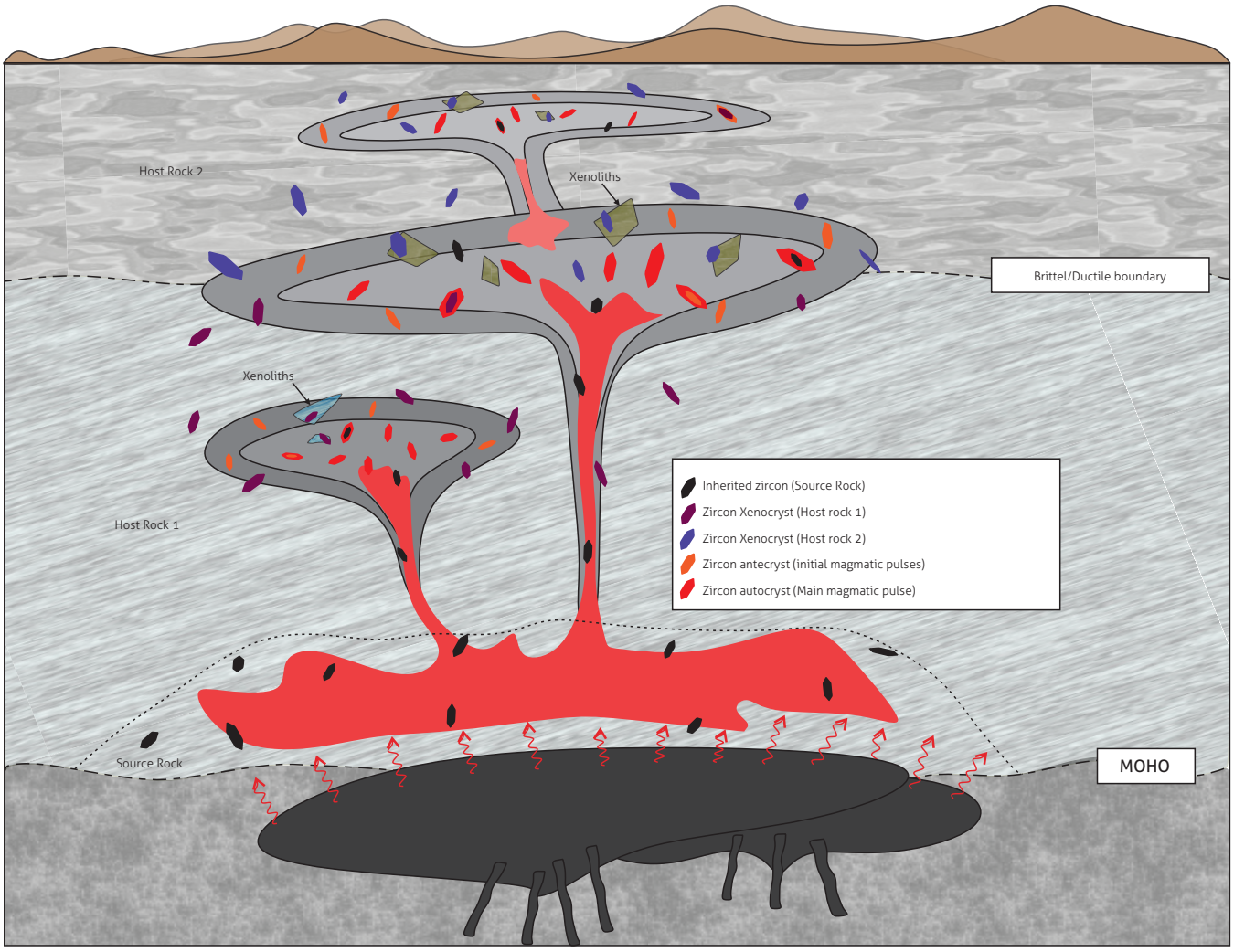

Figure 4. Schematic diagram of the possible types of zircons present in a magmatic system, corresponding to inherited zircons, xenocrysts, anticrysts and autocrysts, according to the criteria by Miller et al. (2007)

phological typology of the crystal (Pupin, 1980); b) classify internal textures using cathodoluminescence images (Corfu et al.,2003); c) cluster the ages obtained from crystals interpreted as xenocrysts, anticrysts and autocrysts; and d) calculate inherited and crystallization ages using the Isoplot (Ludwig, 2009) or IsoplotR (Vermeesch, 2018) programs.

To determine whether the calculated ages are statistically reliable, the statistical parameter mean squared weighted deviation, MSWD (Wendt and Carl, 1991), should be used because this parameter indicates the level of data dispersion (Vermeesch, 2018) and makes it possible to indirectly assess whether individual age weighting and uncertainty represent a single population (Spencer et al., 2016). Accordingly, MSWD = 1 indicates that the calculated age neither underestimates nor overestimates the associated uncertainties; MSWD < 1 indicates overestimated ages, and MSWD > 3 indicates underestimated ages (Spencer et al., 2016; Vermeesch, 2018). Thus, acceptable values of MSWD vary in the range of > 0 to 3, and these values are in turn related to the number of analyses used to calculate the age, as more analyses achieve better MSWD values (see Figure 3 of Spencer et al., 2016). For example, for a number of analyses (or spots) of N = 20, the acceptable MSWD would range from 0.35 to 1.65, for an age calculated with 2σ, which guarantees a reliable age (Spencer et al., 2016). On the other hand, statistically significant ages are those that present a value of P (X^2) 0.05 to 0.95, and this parameter indicates the level of data dispersion with respect to analytical uncertainties around the best-fit line (Vermeesch, 2018).

3.2. Thermobarometry in igneous rocks: emplacement depth

To approximate the emplacement depth of an intrusive body, the magma crystallization pressure and the crystallization temperature near the *solidus* line must be simultaneously estimated (Blundy and Holland, 1990; Holland and Blundy, 1994; Anderson, 1996; Anderson and Smith, 1995; Anderson et al., 2008; Mutch et al., 2016). Various thermobarometers have been proposed in the literature to determine these intensive variables from the composition, equilibrium or saturation of mineral phases present in the intrusive bodies (Table 1). The thermobarometers applied to intrusive rocks are described as follows:

Al-in-Hornblende barometer (Al in Hbl)

This barometer is based on the strong correlation between the total Al content in Hbl and the crystallization pressure of an intrusive (Hammarstrom and Zen, 1986). From this correlation, various equations found in the literature are formulated, generally based on experimental petrology, to estimate the crystallization pressure. The equations differ in the initial experimental parameters, such as the total composition of the host rock, the nature of the fluid phase (H_2O or H_2O-CO_2), the temperature range at which the experiment was performed and the different empirical or experimental calibrations of each equation (Hammarstrom and Zen, 1986; Schmidt, 1992; Anderson and Smith, 1995; Anderson et al., 2008; Mutch et al., 2016).

For a metaluminous granitoid of intermediate to felsic composition with a mineral association of quartz + plagioclase (An_{25-35}) + hornblende + biotite + titanium and iron oxides ± potassium feldspar ± titanite, which was most likely emplaced from 2 kbar to 14 kbar at crystallization temperatures lower than 800 °C, equation 1 (Anderson and Smith, 1995) is applied:

$$P(kbar) = 4.76\ \text{Al-3.01-}\frac{[T°C - 675]}{85} \times$$

$$[0.530\ Al + 0.005294(T°C - 675)] \pm 0.6\ kbar \qquad (1)$$

Applying this barometer requires estimating the crystallization temperature (Anderson and Smith, 1995) because the positive correlation between temperature and $^{[IV]}$Al content in Hbl (Blundy and Holland, 1990) generates overestimated values of pressure at high temperature (>650 °C) (Anderson and Smith, 1995). To use this equation, the authors also recommend ensuring high oxygen fugacity (fO_2) in the system based on Fe/(Fe+Mg) ratios in Hbl ranging from 0.4 to 0.61.

For granitoids with a mineral association of amphibole + plagioclase (An_{15-85}) + biotite + quartz + alkali feldspar + ilmenite/titanite + magnetite + apatite at temperatures near the *solidus* line (725 ± 75 °C), which are emplaced at low pressures (from 2.5 to 0.5 kbar), equation 2 (Mutch et al., 2016) should be used:

$$P\ (kbar) = 0.5 + 0.331(8) \times Al + 0.995(4) \times Al^2 \pm 16\%\ P \qquad (2)$$

Wherein the numbers in parentheses correspond to the uncertainty 1σ expressed in the physical notation with the lowest significant number (Mutch et al., 2016). To correctly apply this equation, the crystallization temperature should also be estimated, thereby ensuring the necessary conditions for its use, which assumes a crystallization temperature of approximately 725 ± 75 °C, as previously mentioned.

Amph+Pl Thermometer

The Amph + Pl thermometer is used to determine the crystallization temperature of a granitoid of variable composition (even with rocks unsaturated in quartz) with a mineral association between amphibole and plagioclase over a temperature range of 400-1000 °C and a pressure range of 1-15 kbar (Holland and Blundy, 1994). This thermometer is based on the equations of equilibrium between edenite + quartz = tremolite + albite (for associations with quartz, termed *thermometer A*) and edenite + albite = richterite + anorthite (for associations without quartz, termed *thermometer B*). This technique considers a non-ideal mixture in both amphibole and plagioclase compositions and calibrates the equations using a database of natural and synthetic amphiboles to reach uncertainties of ± 35-40 °C or higher for iron-rich amphiboles (Holland and Blundy, 1994). The equations (3) and (4) are proposed by the authors.

Iterative calculations using this thermometer and the Al-in-Hbl barometer can provide reliable pressure and temperature ranges in metaluminous granitoids (cf. Anderson et al., 2008).

Thermobarometers based on the composition of calcic amphiboles

A set of barometers and thermometers based on the chemical composition of amphiboles, which is applicable under conditions of temperature raging from 1130 to 800 °C and under a wide pressure range from 22 to 1.3 kbar, have been reported for calc-alkaline and alkaline rocks with calcic amphibole (Ridolfi et al., 2010; Ridolfi and Renzuli, 2012). These thermobarometers are empirically formulated from data in the literature regarding natural and synthetic amphibole compositions, with multivariate least squares analysis of experimental compositions of this mineral (Ridolfi et al., 2010; Ridolfi and Renzuli, 2012).

Thermobarometers based on the clinopyroxene-liquid equilibrium

Thermobarometers based on the clinopyroxene-liquid equilibrium can be used in intrusive rocks of mafic composition under conditions of pressure ranging from 0 to 30 kbar and temperatures ranging from 1100 to 1475 °C (Putirka et al., 1996). These thermobarometers are recommended for rocks that are not granitoids, because mafic rocks are exposed over wide areas in Western Colombia.

Other barometers

In peraluminous granitoids without the required mineral associations to use the Al-in-Hbl barometer and without a suitable composition of calcic amphiboles, pressure can be estimated using empirical garnet + biotite + plagioclase + quartz (Wu et al., 2004a) or garnet + muscovite + plagioclase + quartz (Wu et al., 2004b) barometers developed for metapelitic rocks, which are recommended for granitoids with this mineralogy (Anderson et al., 2008). Similarly, in peraluminous plutons with garnet and muscovite, where muscovite contains celadonite, pressure can be estimated by barometry developed in high-pressure metapelites (cf. Wei and Powell, 2004; 2006; Anderson et al., 2008).

Moreover, the identification of stable mineral phases under specific pressure conditions can constrain the calculation, such

$$\text{Thermometer A: } \frac{\text{-76.95} + 0.79P + Y_{ab} + 39.4X_{Na}^{A} + 22.4X_{Na}^{A} + (41.5 - 2.89\ P)\ .\ X_{Al}^{M_2}}{-0.0650 - \text{R}\ .\ ln\left(\dfrac{27\ .\ X_{\square}^{A}\ .\ X_{Si}^{T_1}\ .\ X_{ab}^{plag}}{256\ .\ X_{Na}^{A}\ .\ X_{Al}^{T_1}}\right)} \quad (3)$$

where the term $Y_{ab} = 0$, if > 0.5; otherwise, $Y_{ab} = 12.0(1 - X_{ab})^2 - 3.0\ kj$; the empty box in $X_{\square}^{A}$ corresponds to the vacancy in the crystallographic site A of amphiboles.

$$\text{Thermometer B: } \frac{78.44 + Y_{ab-an} - 33.6X_{Na}^{M4} - (66.8 - 2.92\ P)\ .X_{Al}^{M2} + 78.5X_{Al}^{T1} + 9.4\ X_{Na}^{A}}{0.0721 - \text{R}\ .\ ln\ \dfrac{27\ .\ X_{Na}^{M4}\ .\ X_{Si}^{T_1}\ .\ X_{an}^{plag}}{64\ .\ X_{Ca}^{M4}\ .\ X_{Al}^{T_1}\ .\ X_{ab}^{plag}}} \quad (4)$$

where the term $Y_{ab-an} = 0$, if $X_{ab} > 0.5$; otherwise, $Y_{ab-an} = 12.0\ (2X_{ab} - 1) + 3.0\ kj$, expressing the temperature as Kelvin, the pressure as kbar, the composition X_i^{Φ} as the molar fraction of element i in mineral phase $^{\Phi}$, and gas constant $R = 0.0083144\ kjK^{-1}mol^{-1}$ (Holland and Blundy, 1994).

as the presence of magmatic epidote, which suggests a pressure > 5 kbar (Zen and Hammarstrom, 1984; Schmidt, 1993). The emplacement depth of an intrusive body can also be estimated when knowing the pressure and temperature conditions at the contact aureole (e.g., garnet + biotite + cordierite equilibrium [cf. Treloar, 1981] and with the aforementioned barometry in peraluminous granitoids applied to the contact rocks [cf. Wu et al., 2004 a, b]). Moreover, the depth of an intrusive body can be qualitatively estimated in terms of epizonal (0-10 km), mesozonal (6-16 km) and catazonal (> 10 km) emplacement by characterizing the type of contact and by describing micro- and mesostructures of the intrusive body and host rock (Buddington, 1959; Paterson et al., 1996), although the resulting ranges should be taken with caution.

Other thermometers

Other thermometers, which can be applied to intrusive bodies of different compositions, are based on the saturation of accessory phases or on the content of the trace elements of these phases (cf. Anderson et al., 2008), such as zircon (Watson and Harrison, 1983) and apatite (Tollari et al., 2006) saturation thermometers and titanium (Ti)-in-zircon (Watson et al., 2006; Ferry and Watson, 2007) and zirconium (Zr)-in-titanite (Hayden et al., 2008) thermometers.

Crystallization temperatures obtained by zircon saturation and Ti-in-zircon thermometers are not always comparable, and the crystallization temperatures tend to be more closely associated with the temperature derived from the Ti-in-zircon method (Harrison et al., 2007) because zircon saturation temperature can be affected by the presence of pre-magmatic zircons (xenocrysts) in the granitic systems that saturate the magma with zircon during the melting process and not during the crystallization process.

The Ti-in-zircon thermometer is based on both empirical and experimental calibration, according to the abundance ratio of titanium in zircon and to its variation as a function of the crystallization temperature, and it is derived from equation 5 (Watson et al., 2006):

$$logTi(ppm)_{zircon} = 5.69 - \left[\frac{3765}{T(K)}\right] \quad (5)$$

However, the substitution of Ti in zircon is related to the activities of TiO_2 and SiO_2. Therefore, a new experimental calibration is required in a temperature range from 1450 to 590 °C, which emphasizes the effect of these activities (Ferry and Watson, 2007):

$$logTi(ppm)_{zircon} = 5.711 - \left[\frac{4800}{T(K)}\right] - log\,(a_{SiO2}) + log\,(a_{TiO2}) \quad (6)$$

In turn, the Zr-in-titanite thermometer was empirically and experimentally calibrated by Hayden et al. (2008), based on experiments at temperatures ranging from 800 to 1000 °C and at pressures ranging from 10 to 24 kbar, and the variation in the Zr abundance in titanite as a function of temperature and pressure is described by using equation 7:

$$logZr(ppm)_{titanite} = 10.52 - \left[\frac{7708}{T(K)}\right] - \left[960 \times \left(\frac{P\ (Gpa)}{T(K)}\right)\right]$$
$$- log\,(a_{SiO2}) - log\,(a_{TiO2}) \quad (7)$$

Table 1. Thermobarometers that are potentially suitable for estimating pressure and temperature in intrusive rocks

Barometer/thermometer	P and/or T conditions	Compositional characteristics	Reference
Al-in-Hlb Barometer	Pressure range = 2-14 kbar	Metaluminous granitoids	Anderson and Smith (1995)
	Pressure < 2.5 kbar	Metaluminous granitoids	Mutch et al. (2016)
Hbl+Pl Thermometer	Pressure range = 1-15 kbar, temperature range = 400-1000 °C	Granitoids with quartz (thermometer A) / Granitoids without quartz (thermometer B)	Holland and Blundy (1994)
Thermobarometers based on the composition of calcic amphiboles	Pressure range = 1.3-22 kbar, temperature range = 1130-800 °C	Calc-alkaline and alkaline rocks	Ridolfi et al., (2010); Ridolfi and Renzulli (2012)
Thermobarometer based on the clinopyroxene-liquid equilibrium	Pressure range = 0-30 kbar, temperature range = 1100-1475 °C	Mafic igneous rocks	Putirka et al. (1996)
Gr+Bt+Pl+Qz barometer	Pressure range = 1-11.4 kbar, temperature range = 515-878 °C	Peraluminous granitoids/ hornfels with this mineralogy	Wu et al. (2004a)
Gr+Ms+Pl+Qz barometer	Pressure range = 1-11.4 kbar, temperature range = 505-745 °C	Peraluminous granitoids/ hornfels and/ or host rock with this mineralogy	Wu et al. (2004b)
Zircon-saturation thermometer	Near-*solidus* temperature	Intermediate to felsic granitoids	Watson and Harrison (1983)
Apatite- saturation thermometer	Near-*liquidus* temperature	Peraluminous granitoids	Tollari et al. (2006)
Ti-in-zircon thermometer	Temperature range = 1450-590 °C	Intermediate to felsic granitoids	Ferry and Watson (2007)
Zr-in-titanite thermometer	Pressure range = 10-24 kbar, temperature range = 800-1000 °C	Intermediate to felsic granitoids	Hayden et al. (2008)

This thermometer may underestimate the temperature if the TiO_2 content is < 1, as expected in common intrusive bodies without rutile (Hayden and Watson, 2007; Anderson et al., 2008). Also, the apatite saturation temperature can be used for peraluminous granitoids (Tollari et al., 2006).

3.3. High-temperature thermochronology: initial cooling age

The interpretation of a cooling age in intrusive rocks is directly related to the concept of closure temperature. Closure temperature is defined as the temperature at which a radiometric system starts to accumulate the daughter isotopes produced by the decay of the parent isotope, which reduces the diffusion loss to almost zero (Dodson, 1973; 1979). Based on this concept, various thermochronometers are sensitive to temperature variations and provide information on the thermal history of the rock, rather than mineral crystallization ages (cf. Dodson, 1973; Zeitler, 1985; Gallagher et al., 1998; Kelley, 2002; Reiners and Brandon, 2006; Peyton and Carrapa, 2013a).

Thus, the cooling ages of intrusive rocks correspond to the ages obtained using thermochronological systems with a closure temperature lower than the crystallization temperature of the intrusive body (cf. Dodson, 1979; Zeitler, 1985; Kelley, 2002; Reiners and Brandon, 2006). The initial cooling ages correspond to the post-emplacement ages that are close to the crystallization age of the intrusive body. To calculate these ages, high-temperature thermochronology is the most suitable approach (cf. Harrison, 1982; Zeitler, 1985; Reiners and Brandon, 2006; Schaen et al., 2020). To clarify, the closure temperatures of the systems will depend on the cooling rate of the rock and on kinetics, geometry, composition and size crystal (cf. Dodson, 1979; Harrison, 1982; Donelick et al., 2005; Reiners and Brandon, 2006; Reiners et al., 2017, pp. 97-101; Oriolo et al., 2018; Bernet et al., 2019).

Among the high-temperature thermochronometers (Figure 3), hornblende and muscovite $^{40}Ar/^{39}Ar$ methods stand out because the radiogenic isotope argon is a noble gas, which can be easily affected by diffusion in the minerals and which is only fully retained when the intrusive rock is already at a cooling stage (Dalrymple and Lanphere, 1969). Furthermore, these thermochronometers have considerably higher closure temperatures than other thermochronometers suitable for calculating initial cooling ages (Harrison, 1982; Zeitler, 1985; Harrison et al., 2009; Reiners et al., 2017, pp. 231-253; Schaen et al., 2020) (Figure 3). In the biotite $^{40}Ar/^{39}Ar$ method, the thermometer is considered to be a low-temperature thermometer (Figure 3) because the closure temperatures range from 330 to 280 °C (cf. Harrison et al., 1985; Grove and Harrison, 1996), thus recording younger cooling ages, which would not correspond to the initial cooling ages of an intrusive rock. The potassium feldspar $^{40}Ar/^{39}Ar$ method shows a wide range of closure temperatures (~350-150 °C) (Figure 3) and frequently contains complex microstructures and degrees of alteration. Thus, the potassium feldspar $^{40}Ar/^{39}Ar$ thermochronometer is not recommended for plutonic and metamorphic rocks and is accordingly more often applied to the geochronology of volcanic rocks (cf. Reiners et al., 2017, p. 240; Schaen et al., 2020).

$^{40}Ar/^{39}Ar$ dating can lead to interpretation problems and ages without geological significance. These caveats are related to a) ^{39}Ar recoil, which disturbs the $^{40}Ar/^{39}Ar$ ratio and the accuracy of age and affects fine-grained minerals and minerals with a high surface/volume ratio (e.g., micas) (cf. Kelley, 2002; Reiners et al., 2017, p. 240; Schaen et al., 2020); b) low K concentrations (~< 2% wt K_2O), which makes it difficult to detect ^{39}Ar, and high Ca/K ratios, which can generate interference problems due to reactions in the reactor, two conditions that affect amphiboles (cf. McDougall and Harrison, 1999; Kelley, 2002; Reiners et al., 2017, p. 241); c) argon loss by diffusion, due to the density of defects in the crystalline structure of the mineral (e.g., fractures) and to edge defects (cf. Dahl, 1996; Kramar et al., 2001; Kelley, 2002; Schaen et al., 2020), and d) argon excess in the minerals resulting from fluid, melt or solid inclusions, with the fluid and melt phases being high reservoirs of ^{40}Ar because the element is highly incompatible (cf. Esser et al., 1997; Boven et al., 2001; Kelley, 2002; Schaen et al., 2020).

Considering the above information, step heating should be used in $^{40}Ar/^{39}Ar$ dating because this approach may show the behavior of a partly open system, the presence of non-radiogenic ^{40}Ar in the sample and the ^{39}Ar recoil associated with the surface of the crystal (cf. Turner, 1970; Kelley, 2002; Reiners et al., 2017, pp. 243-246; Schaen et al., 2020). This technique generates an age spectrum as a function of the degassed fraction of the sample from step heating, in which a spectrum with a significant number of continuous steps and with indistinguishable ages will provide a plateau age, and this age is considered to be a concordant age (cf. Lanphere and Dalrymple, 1971; McDougall and Harrison, 1999; Fleck et al., 1977; Faure and Mensing, 2005; Reiners et al., 2017, pp. 243-246; Schaen et al., 2020). The plateau age should comprise at least 50% of the ^{39}Ar

released, at a 95% confidence level for each age encompassing the plateau age (Fleck et al., 1977), as well as include at least five or more consecutive steps (Schaen et al., 2020).

The spectrum of ages shows the excess of ^{40}Ar in the samples, for example, the excess of ^{40}Ar accumulated through fluid inclusions when released at low temperatures, as well as the excess of ^{40}Ar accumulated through melt or solid inclusions when released at high temperatures, which generates a U- or horseshoe-shaped spectrum of ages with older ages at the ends (cf. Lanphere and Dalrymple, 1971; Wartho et al., 1996; Kelley, 2002). Spectra with discordant ages that do not form plateau ages are also observed and are attributed to ^{40}Ar loss by diffusion, ^{39}Ar recoil or ^{39}Ar excess (cf. Turner, 1970; Boven et al., 2001; Reiners et al., 2017, pp. 243-246; Schaen et al., 2020).

Initial cooling rate

The initial cooling rates can be calculated using the hornblende and muscovite $^{40}Ar/^{39}Ar$ method thanks to the different closure temperatures of these thermochronometers (Figure 3). In this case, the oldest cooling age would be recorded when applying the hornblende $^{40}Ar/^{39}Ar$ method, which has a higher closure temperature (between 550 and 480 °C) (cf. Harrison, 1982) than the muscovite $^{40}Ar/^{39}Ar$ method, which has a relatively lower closure temperature (between 440 and 390 °C) (cf. Harrison et al., 2009), thereby yielding younger ages. By calculating these ages, including the crystallization age, the initial cooling rates of the intrusive rock can be estimated.

This initial cooling rate can be interpreted as a) cooling associated with heat transfer by conduction or advection (cf. Peacock 1989; Zeitler, 1985; Ehlers, 2005), or b) cooling attributed to tectonic exhumation processes that decrease the ambient temperature of the intrusive body (cf. Zeitler, 1985; England and Molnar, 1990; Ring et al., 1999). To infer the process that controlled the initial cooling, the tectonic context in which the intrusive body was emplaced and the physical parameters that describe the heat transfer processes should be considered (Ehlers, 2005). For example, one-dimensional heat diffusion in a given intrusive body could be estimated using equation 8 (Carslaw and Jaeger, 1959; Ehlers, 2005):

$$\frac{\partial T}{\partial t} = K \frac{\partial^2 T}{\partial z^2} \quad (8)$$

where ∂T is the temperature difference between the intrusive body and the host rock, ∂t is the time that the system spends decreasing its temperature, z is the parameter associated with the dimensions of the intrusive body, and K is the thermal diffusivity constant of an intrusive body (approximately 32 km^2/Ma) (Ehlers, 2005). The dimensions of the intrusive body can be estimated with its exposed surface area, field relationships and depth of emplacement, which is combined with geophysical techniques if available (cf. Clarke, 1992; Pitcher, 1997). The variation in temperature as a function of time can be assessed using the previously described thermometers and thermochronometers, including thermobarometry in the host rock, to determine the possible thermal paleogradient.

By applying equation 8 to a one-dimensional model and assuming a flat body shape, the initial temperature of a surface intrusive body with a diameter of 5 km, which affects a host rock at a temperature of 50 °C, decreases from 700 to 500 °C over 100000 years, which is exclusively due to heat conduction processes (Ehlers, 2005). In this model, the intrusive body size (diameter) increases the amount of heat that affects the host rock as its temperature decreases, as well as the duration and distance of the heat source. Under these conditions, an equilibrium should be reached between the temperature of the intrusive body and the host rock, which is controlled by the geothermal gradient of the environment (Ehlers, 2005).

Considering the above information, simple heat transfer models should be applied to identify the prevailing cooling process in each intrusive body, that is, whether cooling results from heat dissipation, from an associated tectonic event or from both (cf. Zeitler, 1985; Ehlers, 2005). For this, it must determine the cooling rates, the closure temperatures of the geothermochronometers, the initial temperatures of both the intrusive body and the host rock (thermobarometry, Table 1) and the relative dimensions of the rock bodies (cf. Clarke, 1992; Pitcher, 1997; Ehlers, 2005).

3.4. Low-temperature thermochronology: cooling/ exhumation age in the upper crust

Low-temperature thermochronology is suitable for studying cooling processes at upper levels in the crust (cf. Gallagher et al., 1998; Farley, 2002; Peyton and Carrapa, 2013a; Reiners et al., 2017, pp. 105-127; Bernet et al., 2019) because this approach includes thermochronometers with closure temperatures lower than 300 °C, equivalent to shallow depths not exceeding 10 km, for a geothermal gradient of 30 °C/km (Figure 3, Table 2). In general, this cooling is generated as rocks move toward the surface through exhumation events resulting from erosion processes or tectonic activity (cf. England and

Molnar, 1990; Brandon et al., 1998; Ring et al, 1999; Reiners and Brandon, 2006; Peyton and Carrapa, 2013a). These ages can be associated with the exhumation ages of the rock body. By combining different thermochronometers (with different closure temperatures), exhumation rates can be estimated and thermal histories can be modeled during the passage of rocky bodies through the upper crust (Reiners and Brandon, 2006; Peyton and Carrapa, 2013a; Reiners et al., 2017, pp. 105-127; Bernet et al., 2019; Nieto-Samaniego et al., 2019).

The most commonly used low-temperature thermochronology techniques (cf. Gallagher et al., 1998; Farley, 2002; Donelick et al., 2005; Reiners and Brandon, 2006; Chew and Spikings, 2015; Bernet et al., 2019) are zircon and apatite (U-Th)/He (ZHe and AHe) and fission track (ZFT and AFT) dating. To correctly apply these thermochronological methods, the concepts of partial retention zone (PRZ), applicable to the (U-Th)/He technique, and partial annealing zone (PAZ), applicable to the fission track technique (Gleadow and Fitzgerald, 1987; Wolf et al., 1998; Brandon et al., 1998; Armstrong, 2005; Reiners and Brandon, 2006; Peyton and Carrapa et al., 2013a; Bernet et al., 2019) should be clarified, in addition to the concept of closure temperature. These additional concepts must be considered because the mineral may experience different cooling processes, including a) constant, monotonic and relatively fast cooling with a temperature that is always decreasing over time, in which case the concept of closure temperature would be applied, thereby assessing the cooling age (Table 2, Figure 5A), and b) variable cooling over time, possibly remaining in the temperature ranges of the PAZ and PRZ, in which case the systems are partly open, thus generating partial reset ages (Table 2, Figure 5B) (cf. Gallagher et al., 1998; Wolf et al.,1998; Brandon et al., 1998; Farley, 2002; Donelick et al., 2005; Reiners and Brandon, 2006; Bernet et al., 2019). Hence, thermochronological systems can follow different cooling paths, and each technique must be adequately applied toward understanding their thermal history and modelling cooling and exhumation rates close to reality (cf. Gallagher et al., 1998; Wolf et al., 1998; Farley, 2002; Reiners and Brandon, 2006; Bernet et al., 2019).

(U-Th)/He dating is based on the accumulation of He particles in zircon and apatite crystals derived from alpha decay in $^{238}U \rightarrow ^{206}Pb$, $^{235}U \rightarrow ^{207}Pb$, and $^{232}Th \rightarrow ^{208}Pb$ decay systems (Wolf et al., 1996). Because He undergoes diffusion processes at high temperatures, He is only retained in the crystal below the closure temperature of each mineral (Figure 3, Table 2), thereby recording the cooling age (Wolf et al., 1996; Farley, 2000; Farley, 2002), or He might be partly accumulated in the partial retention zones (PRZ) established for each thermochronometer (Table 2), whereby the ages would be considered to be partial reset ages (Wolf et al., 1998).

Fission track dating is based on the spontaneous fission of ^{238}U that occurred in the crystalline structure of the minerals that contain U (Fleischer et al., 1975). This fission generates tracks (or damage) in the crystalline structure that are formed constantly over time, as long as they are generated below the closure temperature of each system, because fission tracks can quickly annealed due to solid-state diffusion in high-temperature environments (cf. Gallagher et al., 1998; Donelick et al., 2005; Reiners and Brandon, 2006; Bernet et al., 2019). The density of tracks in a crystal sector and the concentration of ^{238}U make it possible to calculate the age at which the mineral cooled below the closure temperature, according to a thermochronometer (Table 2), as long as the mineral has experienced relatively fast, monotonic and constant cooling at rates of approximately 10 to 100 °C/Ma (cf. Bernet et al., 2019) (Figure 5A). Conversely, if the minerals experienced slow cooling (2 °C/Ma), staying in the range of PAZ temperatures (Table 2, Figure 5b), or overheating due to a thermal event (in intrusive bodies), the tracks can partially annealed, thus recording partial reset ages (cf. Bernet et al., 2019).

Table 2. Closure temperatures and temperatures in the PAZ and PRZ corresponding to the ZFT, ZHe, AFT and AHe methods under average conditions

Thermochronometers	Closure temperature (cooling rate at 10 °C/Ma)	PAZ/PRZ		Reference
		Temp. upper	Temp. lower	
ZFT (zircon with natural radiation damage)	~230 °C	237.9°C	180.5 °C	Bernet et al., (2019) and references therein
ZHe	~190 °C	197 °C	159.2 °C	
AFT	~110 °C	114 °C	61 °C	
AHe	~70 °C	73.2 °C	47.9 °C	
Conditions	Monotonic and relatively fast cooling	Slow cooling or overheating		Cf. Peyton and Carrapa (2013a); Bernet et al. (2019)
Age interpretation	Cooling age	Partial reset age		

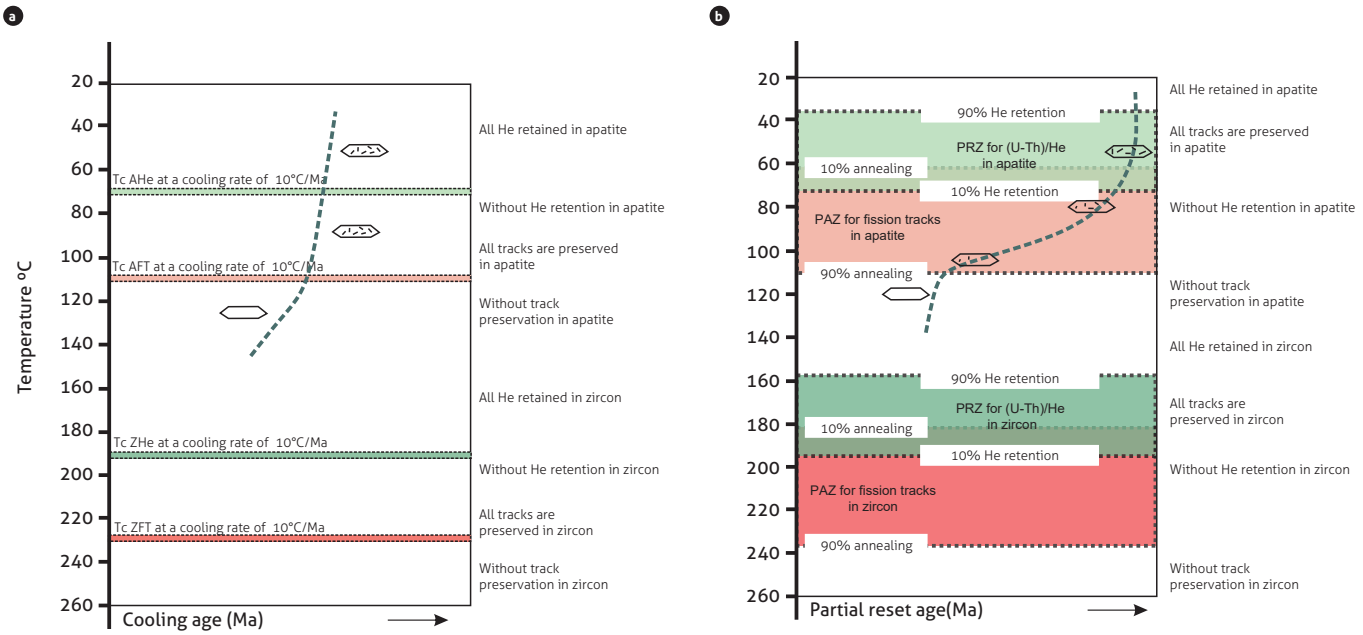

Figure 5. Possible cooling/exhumation curves of paths in the upper crust. a) Relatively fast and monotonic cooling curve; age derived from the closure temperature step (cooling age calculation). b) Slow cooling curve with prolonged passage in the PAZ and PRZ (partial reset age calculation). Temperature thresholds retrieved from Bernet et al. (2019) and references therein (see Table 2).

The AFT technique, in addition to calculating ages, requires studying/understanding of partial annealing degree experienced by the fission track (that is, how much they are shortened or anneling) necessary to know if the sample remained at PAZ temperatures, and for modeling the thermal history of the mineral (Gleadow et al.,1983; Green et al., 1986; Green, Duddy, Laslett et al., 1989; Gallagher et al., 1998; Ketcham et al., 1999; Donelick et al., 2005; Peyton and Carrapa, 2013a). The partial annealing process is mainly controlled by the time-temperature factor that affected the sample and by the direction of tracks with respect to the crystallographic axis, which is correlated with apatite composition (Gleadow et al., 1983; Green et al., 1986; Ketcham et al., 1999; Donelick et al., 2005). The temperature-time factor is determined by the distribution of horizontally confined track lengths, and the crystallographic direction of tracks (and apatite composition) is obtained using kinetic parameters (Gleadow et al., 1983; Green et al., 1986; Green, Duddy, Laslett et al., 1989; Gallagher et al., 1998; Ketcham et al., 1999; Donelick et al., 2005; Peyton and Carrapa, 2013a; Bernet et al., 2019).

The track length distribution method is based on the length-temperature relationship that exists in fission tracks, which could be shortened if the mineral resides within the PAZ temperatures for a significant time, consequently showing a bimodal track length distribution (cf. Green et al., 1986; Donelick et al., 2005; Peyton and Carrapa, 2013a). In this bimodal distribution, the shortest tracks would be the oldest, and the longest tracks would be the most recent, which are formed below the PAZ temperatures (cf. Green et al., 1986; Donelick et al., 2005; Peyton and Carrapa, 2013a).

One of the kinetic parameters is the chemical composition of apatite, which is based on a strong track annealing dependence on the chlorine/fluorine ratio, whereby chlorine-rich apatites are more resistant to track annealing, whereas apatites with fluoride experience faster partial annealing (Green et al., 1985; Barbarand et al., 2003; Donelick et al., 2005). Because determination of the apatite composition requires using destructive or complex and costly analytic techniques, an alternative kinematic parameter is Dpar (Donelick, 1993; Barbarand et al., 2003; Donelick et al., 2005).

Dpar is based on the solubility of the crystal to acid digestion to reveal tracks (etching) and is defined as the diameter of the geometric figure formed by the intersection between the fission track and the polished surface of the crystal; low Dpar values are typical of fluorine apatites, characterized by low annealing temperatures, whereas high Dpar values are common-

ly found in chlorine-rich apatites, characterized by high annealing temperatures (Donelick, 1993; Barbarand et al., 2003; Donelick et al., 2005).

In summary, the distribution of horizontally confined fission track lengths and the kinetic parameter Dpar should be determined to modeling the thermal history of apatite (cf. Green et al., 1985; Donelick, 1993; Gallagher et al., 1998; Barbarand, 2003; Donelick et al., 2005).

In the ZFT method, partial track annealing is controlled by the temperature, time and accumulation of alpha radiation damage (cf. Nasdala et al., 2001; Garver et al., 2002; Rahn et al., 2004; Reiners and Brandon, 2006). Alpha radiation damage occurs during ^{238}U, ^{232}Th and ^{235}U decay and causes changes in the crystallography of the mineral (or metamictisation), as well as color accumulation in zircon due to point defects in the crystals (Nasdala et al., 2001; Garver and Kamp, 2002, Garver et al., 2002; Rahn et al., 2004).

Various studies suggest that zircons with alpha radiation damage are more likely to show partial annealing at temperatures below those faced by zircons with little radiation damage and lower closure temperatures (cf. Brandon et al., 1998; Garver et al., 2002; Rahn et al., 2004; Reiners and Brandon, 2006). Thus, experiments with zircons without alpha radiation damage indicate a closure temperature of approximately 342 °C, at a cooling rate of 10 °C/Ma (Rahn et al., 2004; Reiners and Brandon, 2006), which is considerably higher than that estimated in zircons with natural radiation damage of approximately 230 °C under the same cooling conditions (Brandon et al., 1998) (Table 2).

The closure temperature of zircons with radiation damage is the most recommended value for most geological processes (Brandon et al., 1998; Reiners and Brandon, 2006). In turn, the closure temperature of zircons with zero radiation damage can be applied to environments where zircons show rapid cooling and derive from high-temperature environments (> 350-400 °C), causing little alpha radiation damage to these zircons during closure (Reiners and Brandon, 2006).

Cooling and partial reset age

Various cooling ages can be calculated when an intrusive body experiences a monotonic and relatively fast cooling (Figure 5a). Based on the age vs. closure temperature correlation, the oldest ages would be recorded by ZFT and ZHe (closure temperatures that would vary between approximately 230 and 190 °C, respectively; Table 2), which would provide data on the time when the intrusive passed to a depth ranging from 7 to 5.6 km, assuming a geothermal gradient of 30 °C/km and a surface temperature of 20 °C (cf. Gallagher et al., 1998; Farley, 2002; Reiners and Brandon, 2006; Peyton and Carrapa, 2013a; Bernet et al., 2019). Similarly, the youngest ages would be assessed with AFT and AHe (Table 2), which would indicate the time when the rock body passed at a depth of 3 km with AFT and 1.6 km with AHe (depths close to the surface) (cf. Gallagher et al., 1998; Farley, 2002; Reiners and Brandon, 2006; Peyton and Carrapa, 2013a; Bernet et al., 2019). Therefore, when combining the four thermochronological techniques (or at least two), the cooling ages associated with exhumation processes can be calculated at upper crust levels, as well as the cooling/exhumation rates (cf. Zeitler et al., 1982; Zeitler, 1985; Brandon et al., 1998; Ring et al., 1999; Reiners and Brandon, 2006; Deeken et al., 2006).

Conversely, if the rock body experienced slow and variable cooling (Figure 5) or reheating events, such as through magmatism, hydrothermalism or burial metamorphism, it could reside in the PAZ and PRZ, and the ages calculated using the ZFT, ZHe, AZT and AHe methods would correspond to partial reset ages, whose interpretation requires direct or indirect thermal modeling based on numerical methods (Ehlers, 2005; Peyton and Carrapa, 2013a; Bernet et al., 2019). The literature contains programs and routines for modelling the thermal history of one or more samples based on thermochronological data, such as the HeFty (Ketcham, 2005), QTQt (Gallagher, 2012) and Pecube (Braun et al., 2012) programs. The last program solves the heat transfer equation in three dimensions, which reduces exhumation scenarios, tectonic configurations and time-temperature paths (thermal history) of study samples (cf. Braun et al., 2012).

Considering the above information, two or more low-temperature thermochronometers should be applied when studying the cooling/exhumation processes that intrusive bodies have experienced in their passage through the upper crust, and to thermal modeling when the calculated ages are interpreted as a product of partial reset.

4. Conclusions and final considerations

The path of an intrusive body from emplacement to final exhumation at the surface should be studied to determine its cooling and exhumation history. For this purpose, geothermochronology and thermobarometry techniques can be combined with field observations and relationships.

The present review highlights the application of geothermochronological and thermobarometric methods to determine temperature-time-depth variables in intrusive bodies.

Granitoid emplacement ages are determined using the zircon U-Pb method, and their depths can be estimated with thermobarometry techniques (Table 1). Initial cooling ages can be calculated with high-temperature thermochronology techniques, including hornblende and muscovite $^{40}Ar/^{39}Ar$ methods. Initial cooling rates can also be calculated by combining the crystallization age with the initial cooling age. These cooling rates can be associated with heat diffusion processes (by conduction or advection) or with tectonic events.

Low-temperature thermochronology techniques can be applied to study the passage of intrusive bodies in the upper crust level (<10 km): zircon and apatite fission track (ZFT and AFT) and (U-Th)/He (ZHe and AHe) dating. The ZFT and ZHe thermometers provide data on cooling/exhumation ages at depths ranging approximately from 8 to 6 km (assuming a geothermal gradient of 30 °C/km), and AFT and AHe thermometers record cooling/exhumation ages at near-surface depths (approximately from 4 to 2 km). If the mineral has remained in the PAZ and/or PRZ zones, the calculated ages are considered to be partial reset ages and require thermal modeling for correct interpretation. Two or more low-temperature thermochronology techniques should be combined to calculate exhumation rates at upper crust levels and their possible correlations with tectonic events.

The different techniques proposed in this review may present sources of uncertainty that are not normally included in the error propagation calculation, such as sampling bias, number of statistically representative data, human errors in laboratory work and interlaboratory standard calibration errors, which increase the uncertainty around the final curve or path.

Finally, establishing the cooling/exhumation history of an intrusive body is crucial for understanding the thermal and tectonic evolution of a region. Furthermore, determining the cooling and exhumation rates helps to limit the main tectonic pulses associated with the construction of an orogenic belt or with its collapse during crustal evolution.

Acknowledgements

This study was conducted by the Tectonics Group of the Technical Dirección técnica de Geociencias Básicas of the Servicio Geológico Colombiano (SGC) within the framework of the project entitled *Modelo Tectónico de Colombia* [Tectonic Model of Colombia]. We would like to sincerely thank the anonymous reviewers for their valuable comments and suggestions, which helped to improve the manuscript. We also thank geologists Carlos Augusto Quiroz Prada and Ana María Patiño for their important suggestions and technical comments.

References

Anderson, J. (1996). Status of thermobarometry in granitic batholiths. *Earth and Environmental Science Transactions of the Royal Society of Edinburgh*, *87*(1-2), 125-138. https://doi.org/10.1017/S0263593300006544

Anderson, J., & Smith, D. (1995). The effects of temperature and $f0_2$ on the Al-in-hornblende barometer. *American Mineralogist*, *80*, 549-559. https://doi.org/10.2138/am-1995-5-614

Anderson, J., Barth, A., & Young, E. (1988). Mid-crustal Cretaceous roots of Cordilleran metamorphic core complexes. *Geology*, *16*(4), 366-369. https://doi.org/10.1130/0091-7613(1988)016<0366:MCCROC>2.3.CO;2

Anderson, J., Barth, A., Wooden, J., & Mazdab, F. (2008). Thermometers and thermobarometers in granitic systems. *Reviews in Mineralogy and Geochemistry*, *69*(1), 121-142. https://doi.org/10.2138/rmg.2008.69.4

Armstrong, F. (2005). Thermochronometers in sedimentary basins. *Reviews in Mineralogy and Geochemistry*, *58*, 499-525. https://doi.org/10.2138/rmg.2005.58.19

Barbarand, J., Carter, A., Wood, I., & Hurford, T. (2003). Compositional and structural control of fission-track annealing in apatite. *Chemical Geology*, *198*, 107-137. https://doi.org/10.1016/S0009-2541(02)00424-2

Bernet, M., Piraquive, A., Urueña, C., López Isaza, J., Bermúdez, M., Zuluaga, C., Amaya, S., & Villamizar, N. (2019). Multidisciplinary petro-geo-thermochronological approach to ore deposit exploration. *Ore Geology Reviews*, *112*, 1-17. https://doi.org/10.1016/j.oregeorev.2019.103017

Bernet, M., Van der Beek, P., Pik, R., Huyghe, P., Mugnier, J. L., Labrin, E., & Szulc, A. (2006). Miocene to recent exhumation of the central Himalaya determined fromcombined detrital zircon fission-track and U/Pb analysis of Siwalik sediments, Western Nepal. *Basin Research*, *18*(4), 393-412. https://doi.org/10.1111/j.1365-2117.2006.00303.x

Blundy, J., & Holland, T. (1990). Calcic amphibole equilibria and a new amphibole-plagioclase geothermometer. *Contributions to Mineralogy and Petrology*, *104*, 208-224. https://doi.org/10.1007/BF00306444

Boven, A., Pasteels, P., Kelley, S., Punzalan, L., Bingen, B., & Demaiffe, D. (2001). $^{40}Ar/^{39}Ar$ study of plagioclases from the Rogaland anorthosite complex (SW Norway); an attempt to understand argon ages in plutonic plagioclase. *Chemical Geology*, *176*(1-4), 105-135. https://doi.org/10.1016/S0009-2541(00)00372-7

Brandon, M., Roden Tice, M., & Garver, J. (1998). Late Cenozoic exhumation of the Cascadia accretionary wedge in the Olympic Mountains, Northwest Washington State. *GSA Bulletin*, *110*(8), 985-1009. https://doi.org/10.1130/0016-7606(1998)110<0985:LCEOTC>2.3.CO;2

Braun, J., Van Der Beek, P., Valla, P., Robert, X., Herman, F., Glotzbach, C., Pedersen, V., Perry, C., Simon-Labric, T., & Prigent, C. (2012). Quantifying rates of landscape evolution and tectonic processes by thermochronology and numerical modeling of crustal heat transport using Pecube. *Tectonophysics*, *524*, 1-28. https://doi.org/10.1016/j.tecto.2011.12.035

Buddington, A. (1959). Granite emplacement with special reference to North America. *Bulletin of The Geological Society of America*, *70*, 571-747. https://doi.org/10.1130/0016-7606(1959)70[671:GEWSRT]2.0.CO;2

Caggianelli, A., Prosser, G., & Del Morro, A. (2000). Cooling and exhumation history of deep-seated and shallowlevel, late Hercynian granitoids from Calabria. *Geological Journal*, *35*, 33-42. https://doi.org/10.1002/(SICI)1099-1034(200001/03)35:1<33::AID-GJ836>3.0.CO;2-U

Cardona, A., Valencia, V., Weber, M., Duque, J., Montes, C., Ojeda, G., Reiners, P., Domanik, K., Nicolescu, S., & Villagómez, D. (2011). Transient Cenozoic tectonic stages in the southern margin of the Caribbean plate: U-Th/He thermochronological constraints from Eocene plutonic rocks in the Santa Marta massif and Serranía de Jarara, Northern Colombia. *Geological Acta*, *9*(3-4), 445-466. https://doi.org/10.1344/105.000001739

Carroll, M., & Wyllie, P. (1990). The system tonalite-H_2O at 15 kbar and the genesis of calc-alkaline magmas. *American Mineralogist*, *75*(3-4), 345-357.

Carslaw, H., & Jaeger, J. (1959). *Conduction of heat in solids*. Clarendon Press. https://doi.org/10.2307/3610347

Cherniak, D., & Watson, E. (2001). Pb diffusion in zircon. *Chemical Geology*, *172*(1-2), 5-24. https://doi.org/10.1016/S0009-2541(00)00233-3

Chew, D., & Spikings, R. (2015). Geochronology and thermochronology using apatite: Time and temperature lower crust to surface. *Elements*, *11*, 189-194. https://doi.org/10.2113/gselements.11.3.189

Clarke, D. (1992). *Granitoid rocks*. Chapman y Hall. Topics in the Earth Sciences, 7.

Coleman, D., Gray, W., & Glazner, A. (2004). Rethinking the emplacement and evolution of zoned plutons: Geochronologic evidence for incremental assembly of the Tuolumne Intrusive Suite, California. *Geology*, *32*(5), 433-436. https://doi.org/10.1130/G20220.1

Corfu, F., Hanchar, J., Hoskin, P., & Kinny, P. (2003). Atlas of zircon textures. *Reviews in Mineralogy and Geochemistry*, *53*(1), 469-500. https://doi.org/10.2113/0530469

Corrigan, J. (1991). Inversion of apatite fission track data for thermal history information. *Journal of Geophysical Research*, *96*(B6), 10347-10360. https://doi.org/10.1029/91JB00514

Cortés Calderón, E. (2015). *Geochemical behavior and emplacement conditions of the Ibagué Batholith: Regional implications* (tesis de grado), Universidad de los Andes.

Dahl, P. (1996). The crystal-chemical basis for Ar retention in micas: Inferences from interlayer partitioning and implications for geochronology. *Contributions to Mineralogy and Petrolpgy*, *123*, 22-39. https://doi.org/10.1007/s004100050141

Dalrymple, G., & Lanphere, M. (1969). *Potassium-argon dating: Principles, techniques and applications to geochronology*. Freeman.

Deeken, A. S. (2006). Development of the Southern Eastern Cordillera, NW Argentina, constrained by apatite fission track thermochronology: From early Cretaceous extension to middle Miocene shortening. *Tectonics*, *25*(6). https://doi.org/10.1029/2005TC001894

Dodson, M. (1973). Closure temperature in cooling geochronological and petrological systems. *Contributions to Mineralogy and Petrology*, *40*(3), 259-274. https://doi.org/10.1007/BF00373790

Dodson, M. (1979). Theory of cooling ages. En E. Jäger y J. C. Hunziker (eds.), *Lectures in isotope geology* (pp. 194-202), Springer. https://doi.org/10.1007/978-3-642-67161-6_14

Donelick, R. (1993). Apatite etching characteristics versus chemical composition. *Nuclear Tracks and Radiation Measurements*, *21*(604), 1359-0189

Donelick, R., O'Sullivan, P., & Ketcham, R. (2005). Apatite fission-track analysis. *Reviews in Mineralogy and Geochemistry*, *58*, 49-94. https://doi.org/10.2138/rmg.2005.58.3

Ehlers, T. (2005). Crustal thermal processes and the interpretation of thermochronometer data. *Reviews in Mineralogy and Geochemistry*, *58*(1), 315-350. https://doi.org/10.2138/rmg.2005.58.12

England, P., & Molnar, P. (1990). Surface uplift, uplift of rocks, and exhumation of rocks. *Geology*, *18*(12), 1173-1177. https://doi.org/10.1130/0091-7613(1990)018<1173:SUUORA>2.3.CO;2

Esser, R., McIntosh, W., Heizler, M., & Kyle, P. (1997). Excess argon in melt inclusions in zero-age anorthoclase feldspar from Mt Erebus, Antarctica, as revealed by the $^{40}Ar/^{39}Ar$ method. *Geochimica et Cosmochimica Acta*, *61*(18), 3789-3801. https://doi.org/10.1016/S0016-7037(97)00287-1

Farley, K. (2000). Helium diffusion from apatite: General behavior as illustrated by Durango fluorapatite. *Journal of Geophysical Research: Solid Earth*, *105*(B2), 2903-2914. https://doi.org/10.1029/1999JB900348

Farley, K. (2002). (U-Th)/He Dating: Techniques, calibrations, and applications. *Reviews in Mineralogy and Geochemistry*, *47*(1), 819-844. https://doi.org/10.2138/rmg.2002.47.18

Faure, G., & Mensing, T. (2005). *Isotopes: Principles and applications*. John Wiley & Sons.

Ferry, J., & Watson, E. (2007). New thermodynamic models and revised calibrations for the Ti-in-zircon and Zr-in-rutile thermometers. *Contribution to Mineralogy and Petrology*, *154*, 429-437. https://doi.org/10.1007/s00410-007-0201-0

Fleck, R., Sutter, J., & Elliot, D. (1977). Interpretation of discordant ^{40}Ar-^{39}Ar age-spectra of Mesozoic tholeiites from Antarctica. *Geochimica et Cosmochimica Acta*, *41*, 15-32.

Fleischer, R., Price, P., & Walker, R. (1975). *Nuclear tracks in solids: Principles and applications.* University of California Press.

Foster, D., Miller, C., Harrison, T., & Hoisch, T. (1992). $^{40}Ar/^{39}Ar$ thermochronology and thermobarometry of metamorphism, plutonism, and tectonic denudation in the Old Woman Mountains area, California. *GSA Bulletin*, *104*, 176-191. https://doi.org/10.1130/0016-7606(1992)104<0176:AATATO>2.3.CO;2

Foster, D., Schafer, C., Fanning, C., & Hyndman, D. (2001). Relationships between crustal partial melting, plutonism, orogeny, and exhumation: Idaho-Bitterroot batholith. *Tectonophysics*, *342* (3-4), 313-350. https://doi.org/10.1016/S0040-1951(01)00169-X

Gallagher, K. (2012). Transdimensional inverse thermal history modeling for quantitative thermochronology. *Journal of Geophysical Research: Solid Earth*, *117*(B2). https://doi.org/10.1029/2011JB008825

Gallagher, K., Brown, R., & Johnson, C. (1998). Fission track analysis and its applications to geological problems. *Annual Review of Earth and Planetary Sciences*, *26*, 519-572. https://doi.org/10.1146/annurev.earth.26.1.519

Garver, J. I., & Kamp, P. J. (2002). Integration of zircon color and zircon fission-track zonation patterns in orogenic belts: Application to the Southern Alps, New Zealand. *Tectonophysics*, *349*(1-4), 203-219. https://doi.org/10.1016/S0040-1951(02)00054-9

Garver, J. I., Riley, B. C. D., & Wang, G. (2002). Partial resetting of fission tracks in detritai zircon. *Geotemas*, (4), 73-76.

George, P. (1993). *Tectonic implications of fission-track thermochronology and amphibole thermobarometry studies of the Northern Peninsular Ranges Batholith, Southern California* (tesis Ph. D.), The Louisiana State University.

Gil Rodríguez, J. (2014). Petrology of the Betulia Igneous Complex, Cauca, Colombia. *Journal of South American Earth Sciences*, *56*, 339-356. https://doi.org/10.1016/j.jsames.2014.09.016

Gleadow, A., & Fitzgerald, P. (1987). Uplift history and structure of the Transantarctic Mountains: New evidence from fission track dating of basement apatites in the Dry Valleys area, Southern Victoria Land. *Earth and Planetary Science Letters*, *82*, 1-14.

Gleadow, I., Duddy, I., & Lovering, J. (1983). Fission track analysis: A new tool for the evaluation of thermal histories and hydrocarbon potential. *The APPEA Journal*, *23*(1), 93-102. https://doi.org/10.1071/AJ82009

Glorie, S., Alexandrov, I., Nixon, A., Jepson, G., Gillespie, J., & Jahn, B.-M. (2017). Thermal and exhumation history of Sakhalin Island (Russia) constrained by apatite U-Pb and fission track thermochronology. *Journal of Asian Earth Sciences*, *143*, 326-342. https://doi.org/10.1016/j.jseaes.2017.05.011

Gómez, J., Montes, N., Alcárcel, F., & Ceballos, J. (2015). Catálogo de dataciones radiométricas de Colombia en ArcGIS y Google Earth. En J. Gómez, & M. F. Almanza (eds.), *Compilando la geología de Colombia: Una visión a 2015*. Publi-

caciones Geológicas Especiales, vol. 33. Servicio Geológico Colombiano.

Green, P., Duddy, I., Gleadow, A., & Lovering, J. (1989). *Apatite fission track analysis as palaeotemperature indicator for hydrocarbon exploration.* En N. D. Naeser & T. H. McCulloh (eds.) *Thermal history of sedimentary* (pp. 181-195), Springer-Verlag. https://doi.org/10.1007/978-1-4612-3492-0_11

Green, P., Duddy, I., Gleadow, A., Tingate, P., & Laslett, G. (1985). Fission-track annealing in apatite: Track length measurements and the form of the Arrhenius plot. *Nuclear Tracks and Radiation Measurements*, *10*(3), 323-328. https://doi.org/10.1016/0735-245X(85)90121-8

Green, P., Duddy, I., Gleadow, A., Tingate, P., & Laslett, G. (1986). Thermal annealing of fission tracks in apatite: 1. A qualitative description. *Chemical Geology* (Isotope Geoscience Section), *59*, 237-253. https://doi.org/10.1016/0168-9622(86)90074-6

Green, P., Duddy, I., Laslett, G., Hegarty, K., Gleadowa, A., & Lovering, J. (1989). Thermal annealing of fission tracks in apatite: 4. Quantitative modelling techniques and extension to geological timescales. *Chemical Geology*, *79*: 155-182. https://doi.org/10.1016/0168-9622(89)90018-3

Grove, M., & Harrison, T. (1996). ^{40}Ar* diffusion in Fe-rich biotite. *American Mineralogist*, *81*(7-8), 940-951. https://doi.org/10.2138/am-1996-7-816

Hammarstrom, J., & Zen, E.-A. (1986). Aluminum in hornblende: An empirical igneous geobarometer. *American Mineralogist*, *71*, 1297-1313.

Harrison, T. (1982). Diffusion of ^{40}Ar in hornblende. *Contributions to Mineralogy and Petrology*, *78*(3), 324-331. https://doi.org/10.1007/BF00398927

Harrison, T., Armstrong, R., Naeser, C., & Harakal, J. (1979). Geochronology and thermal history of the Coast Plutonic Complex, near Prince Rupert, British Columbia. *Canadian Journal of Earth Sciences*, *16*(3), 400-410. https://doi.org/10.1139/e79-038

Harrison, T., Celerier, J., Aikman, A., Hermann, J., & Heizler, M. (2009). Diffusion of ^{40}Ar in muscovite. *Geochimica et Cosmochimica Acta*, *73*(4), 1039-1051. https://doi.org/10.1016/j.gca.2008.09.038

Harrison, T., & Clarke, G. (1979). A model of the thermal effects of intrusion and uplift as applied to Quottoon pluton British Columbia. Canadian *Journal of Earth Sciences*, *16*(3), 411-420. https://doi.org/10.1139/e79-039

Harrison, T., Duncan, I., & Mcdougall, I. (1985). Diffusion of ^{40}Ar in biotite: Temperature, pressure and compositional effects. *Geochimica et Cosmochimica Acta*, *49*(11), 2461-2468. https://doi.org/10.1016/0016-7037(85)90246-7

Harrison, T., Watson, E., & Aikman, A. (2007). Temperature spectra of zircon crystallization in plutonic rocks. *Geology*, *35*(7), 635-638. https://doi.org/10.1130/G23505A.1

Hayden, L. A., & Watson, E. B. (2007). Rutile saturation in hydrous siliceous melts and its bearing on Ti-thermometry of quartz and zircon. *Earth and Planetary Science Letters*, *258*, 561-568. https://doi.org/10.1016/j.epsl.2007.04.020

Hayden, L., Watson, E., & Wark, D. (2008). A thermobarometer for sphene. *Contributions to Mineralogy and Petrology*, *155*(4), 529-540. https://doi.org/10.1007/s00410-007-0256-y

Holland, T., & Blundy, J. (1994). Non-ideal interactions in calcic amphiboles and their bearing on amphibole-plagioclase thermometry. *Contributions to Mineralogy and Petrology*, *116*, 433-447. https://doi.org/10.1007/BF00310910

Hunziker, J., Desmons, J., & Hurford, A. (1992). *Thirty-two years of geochronological work in the Central and Western Alps: A review on seven maps*. Mémoires de Géologie (Lausanne), 13.

Hurford, A. (1986). Cooling and uplift patterns in the Lepontine Alps South Central Switzerland and an age of vertical movement on the Insubric fault line. *Contributions to Mineralogy and Petrology*, *92*, 413-427. https://doi.org/10.1007/BF00374424

Kelley, S. (2002). K-Ar and Ar-Ar Dating. *Reviews in Mineralogy and Geochemistry*, *47*(1), 785-818. https://doi.org/10.2138/rmg.2002.47.17

Ketcham, R. (2005). Forward and inverse modeling of low-temperature thermochronometry data. *Reviews in Mineralogy and Geochemistry*, *58*(1), 275-314. https://doi.org/10.2138/rmg.2005.58.11

Ketcham, R., Donelick, R., & Carlson, W. (1999). Variability of apatite fission-track annealing kinetics: III. Extrapolation to geological time scales. *American Mineralogist*, *84*, 1235-1255. https://doi.org/10.2138/am-1999-0903

Kramar, N., Cosca, M., & Hunziker, J. (2001). Heterogeneous Ar-^{40}* distributions in naturally deformed muscovite: In situ UV-laser ablation evidence for micro structurally controlled intra-grain diffusion. *Earth and Planetary Science Letters*, *192*(3), 377-388. https://doi.org/10.1016/S0012-821X(01)00456-3

Lanphere, M., & Dalrymple, G. (1971). A test of the $^{40}Ar/^{39}Ar$ age spectrum technique on some terrestrial material. *Earth and Planetary Science Letters*, *12*, 359-372. https://doi.org/10.1016/0012-821X(71)90020-3

León, S., Cardona, A., Parra, M., Sobel, E., Jaramillo, J., Glodny, J., Valencia, V. A., Chew, D., Montel, C., Posada, G., Monsalve, G., & Pardo Trujillo, A. (2018). Transition from collisional to subduction-related regimes: An example from Neogene Panama-Nazca-South America interactions. *Tectonics*, *37*, 119-139. https://doi.org/10.1002/2017TC004785

Ludwig, K. (2009). *User's manual for Isoplot 3.7: A geochronological toolkit for Microsoft Excel*. Special Publication n.° 4. Geochronology Center.

Martínez, L., & Zuluaga, C. (2010). Thermal modeling of pluton emplacement and associated contact metamorphism: Parashi stock emplacement in the Serranía de Jarara (alta Guajira, Colombia). *Earth Sciences Research Journal*, *14*(2), 145-152.

McDougall, I., & Harrison, T. (1999). *Geochronology and thermochronology by the $^{40}Ar/^{39}Ar$ method*. Oxford University Press.

McInnes, B., Farley, K., Sillitoe, R., & Kohn, B. (1999). Application of apatite (U-Th)/He thermochronometry to the determination of the sense and amount of vertical fault displacement at the Chuquicamata porphyry copper deposit, Chile. *Economic Geology*, *94*(6), 937-947. https://doi.org/10.2113/gsecongeo.94.6.937

Miller, J., Matzel, J., Miller, C., Burguess, S., & Miller, R. (2007). Zircon growth and recycling during the assembly of large, composite arc plutons. *Journal of Volcanology and Geothermal Research*, *167*, 282-299. https://doi.org/10.1016/j.jvolgeores.2007.04.019

Mutch, E., Blundy, J., Tattitch, B., Cooper, F., & Brooker, R. (2016). An experimental study of amphibole stability in low-pressure granitic magmas and a revised Al-in-hornblende geobarometer. *Contributions to Mineralogy and Petrology*, *171*(85), 1-27. https://doi.org/10.1007/s00410-016-1298-9

Nasdala, L., Wenzel, M., Vavra, G., Irmer, G., Wenzel, T., & Kober, B. (2001). Metamictisation of natural zircon: Accumulation versus thermal annealing of radioactivity-induced damage. *Contributions to Mineralogy and Petrology*, *141*(2), 125-144. https://doi.org/10.1007/s004100000235

Nieto Samaniego, A., Olmos Moya, M., Levresse, G., Alaniz Álvarez, S., Abdullin, F., Pilar Martínez, A., & Xu, S. (2019). Thermocronology and exhumation rates of granitic intrusions at Mesa-Central, Mexico. *International Geology Review*, *62*(3), 311-319. https://doi.org/10.1080/00206814.2019.1602789

Oriolo, S., Wemmer, K., Oyhantçabal, P., Fossen, H., Schulz, B., & Siegesmund, S. (2018). Geochronology of shear zones; A review. *Earth-Science Reviews*, *185*, 665-683. https://doi.org/10.1016/j.earscirev.2018.07.007

Parada, M., Féraud, G., Fuentes, F., Aguirre, L., Morata, D., & Larrondo, P. (2005). Ages and cooling history of the Early Cretaceous Caleu pluton: Testimony of a switch from a rifted to a compressional continental margin in central Chile. *Journal of the Geological Society*, *162*, 205, 273-287. https://doi.org/10.1144/0016-764903-173

Paterson, S., Fowler, T., & Miller, R. (1996). Pluton emplacement in arcs: A crustal-scale exchange process. *Earth and Environmental Science Transactions of The Royal Society of Edinburgh*, *87*(1-2), 115-123. https://doi.org/10.1017/S0263593300006532

Peacock, S. (1989). Thermal modeling of metamorphic pressure-temperature-time paths: A forward approach. *Metamorphic Pressure-Temperature-Time Paths*, *7*, 57-102. https://doi.org/10.1029/SC007p0057

Peyton, S., & Carrapa, B. (2013a). An introduction to low-temperature thermochronologic techniques, methodology, and applications. En C. Knight, J. Cuzella & L. D. Cress (eds.), *Application of structural methods to Rocky Mountain hydrocarbon exploration and development* (pp. 15-36), AAPG Studies in Geology, 65. https://doi.org/10.1306/13381688St653578

Peyton, S., & Carrapa, B. (2013b). An overview of low-temperature thermochronology in the Rocky Mountains and its application to petroleum system analysis. En C. Knight, J. Cuzella & L. D. Cress (eds.), *Application of structural methods to Rocky Mountain hydrocarbon exploration and development* (pp. 37-70), AAPG Studies in Geology, 65. https://doi.org/10.1306/13381689St653578

Pitcher, W. (1997). *The nature and origin of granite*. Springer Science+Business Media Dordrecht. https://doi.org/10.1007/978-94-011-5832-9

Pupin, J. (1980). Zircon and granite petrology. *Contributions to Mineralogy and Petrology*, *73*(3), 207-220. https://doi.org/10.1007/BF00381441

Putirka, K., Johnson, M., Kinzler, R., Longhi, J., & Walker, D. (1996). Thermobarometry of mafic igneous rocks based

on clinopyroxene-liquid equilibria, 0-30 kbar. *Contributions to Mineralogy and Petrology*, *123*, 92-108. https://doi.org/10.1007/s004100050145

Rahn, M. K., Brandon, M. T., Batt, G. E., & Garver, J. I. (2004). A zero-damage model for fission-track annealing in zircon. *American Mineralogist*, *89*(4), 473-484. https://doi.org/10.2138/am-2004-0401

Reiners, P., & Brandon, M. (2006). Using thermochronology to understand orogenic erosion. *Annual Review of Earth and Planetary Sciences*, *34*, 419-466. https://doi.org/10.1146/annurev.earth.34.031405.125202

Reiners, P., Carlson, R., Renne, P., Cooper, M., Granger, D., McLean, N., & Schoene, B. (2017). *Geochronology and thermochronology*. John Wiley & Sons. https://doi.org/10.1002/9781118455876

Restrepo Moreno, S., Foster, D., Bernet, M., Min, K., & Noriega, S. (2019). Morphotectonic and orogenic development of the Northern Andes of Colombia: A low-temperature thermochronology perspective. En F. Cediel, R. P. Shaw (eds.), *Geology and tectonics of Northwestern South America,* Frontiers in Earth Sciences. https://doi.org/10.1007/978-3-319-76132-9_11

Restrepo Moreno, S., Foster, D., Stockli, D., & Parra Sánchez, L. (2009). Long-term erosion and exhumation of the "Altiplano Antioqueño", Northern Andes (Colombia) from apatite (U-Th)/He thermochronology. *Earth and Planetary Science Letters*, *278*(1-2), 1-12. https://doi.org/10.1016/j.epsl.2008.09.037

Ridolfi, F., & Renzulli, A. (2012). Calcic amphiboles in calc-alkaline and alkaline magmas: Thermobarometric and chemometric empirical equations valid up to 1130 °C and 2.2 GPa. *Contribution to Mineralogy and Petrology*, *163*, 877-895. https://doi.org/10.1007/s00410-011-0704-6

Ridolfi, F., Renzulli, A., & Puerini, M. (2010). Stability and chemical equilibrium of amphibole in calc-alkaline magmas: An overview, new thermobarometric formulations and application to subduction-related volcanoes. *Contribution to Mineralogy and Petrology*, *160*(1), 45-66. https://doi.org/10.1007/s00410-009-0465-7

Ring, U., Brandon, M., Willett, S., & Lister, G. (1999). *Exhumation processes*. Special Publications, 154, Geological Society. https://doi.org/10.1144/GSL.SP.1999.154.01.01

Sáenz, E. (2003). *Fission track thermochronology and denudational response to tectonics in the north of The Colombian Central Cordillera* (tesis de maestría), Shimane University.

Sáenz, E., Paucar, C., & Restrepo, J. (1996). Estudio de la evolución térmica del Batolito Antioqueño por huellas de fisión. 7th Congreso Colombiano de Geología, Bogotá.

Schaen, A. J., Jicha, B. R., Hodges, K. V., Vermeesch, P., Stelten, M. E., Mercer, C. M. Phillips, D., Rivera, T., Jourdan, F., Matchan, E., Hemming, S., Morgan, L., Kelley, S., Cassata, W., Heizler, M., Vasconcelos, P., Benowitz, J., Koppers, A., Mark, D., Niespolo, E., … Singer, H. (2020). Interpretingandreporting40Ar/39Ar geochronologicdata. *GSA Bulletin*. https://doi.org/10.1130/B35560.1

Schmidt, M. (1992). Amphibole composition in tonalite as a function of pressure: An experimental calibration of the AI-in-hornblende barometer. *Contributions to Mineralogy and Petrology*, *110*, 304-310. https://doi.org/10.1007/BF00310745

Schmidt, M. (1993). Phase relations and compositions in tonalite as a function of pressure: An experimental study at 650 C. *American Journal of Science*, *293*, 1011-1011.

Spencer, C. J., Kirkland, C. L., & Taylor, R. J. (2016). Strategies towards statistically robust interpretations of in situ U-Pb zircon geochronology. *Geoscience Frontiers*, *7*(4), 581-589. https://doi.org/10.1016/j.gsf.2015.11.006

Tollari, N., Toplis, M., & Barnes, S.-J. (2006). Predicting phosphate saturation in silicic magmas: An experimental study of the effects of melt composition and temperature. *Geochimica et Cosmochimica Acta*, *70*, 1518-1536. https://doi.org/10.1016/j.gca.2005.11.024

Treloar, P. (1981). Garnet-biotite-cordierite thermometry and barometry in the Cashel thermal aureole, Connemara, Ireland. *Mineralogical Magazine*, *44*, 183-189. https//doi.org/10.1180/minmag.1981.044.334.11

Turner, G. (1970). $^{40}Ar/^{39}Ar$ dating of lunar rock samples. *Science*, *167*, 466-468.

Van der Lelij, R., Spikings, R., & Mora, A. (2016). Thermochronology and tectonics of the Mérida Andes and the Santander Massif, NW South America. *Lithos*, 248-251, 220-239. https://doi.org/10.1016/j.lithos.2016.01.006

Vermeesch, P. (2018). IsoplotR: A free and open toolbox for geochronology. *Geoscience Frontiers*, *9*(5), 1479-1493. https://doi.org/10.1016/j.gsf.2018.04.001

Villagómez, D., & Spikings, R. (2013). Thermochronology and tectonics of the Central and Western Cordilleras of Colombia: Early Cretaceous-Tertiary evolution of the Northern Andes. *Lithos*, *160*(161), 228-249. https://doi.org/10.1016/j.lithos.2012.12.008

Villagómez, D., Spikings, R., Mora, A., Guzmán, G., Ojeda, G., Córtes, E., & Van der Lelij, R. (2011). Vertical tectonics at a continental crust oceanic plateau plate boundary zone: Fission track thermochronology of the Sierra Nevada de Santa Marta, Colombia. *Tectonics*, *30*, 1-18. https://doi.org/10.1029/2010TC002835

Wagner, G., Reimer, G., & Jager, E. (1977). Cooling ages derived by apatite fission-track, with Rb-Sr and K-Ar dating: The uplift and cooling history of the Central Alps. *Memorie degli Istituti di Geologia e Mineralogia dell' Universita di Padova*, *30*(28), 1-27.

Wartho, J., Rex, D., & Guise, P. (1996). Excess argon in amphiboles linked to greenschist facies alteration in Kamila amphibolite belt, Kohistan island arc system, Northern Pakiston: Insights from 40Ar/39Ar step-heating and acid leaching experiments. *Geological Magazine*, *133*, 595-609. https://doi.org/10.1017/S0016756800007871

Watson, E., & Harrison, T. (1983). Zircon saturation revisited' temperature and composition effects in a variety of crustal magma types. *Earth and Planetary Science Letters*, *64*, 295-304. https://doi.org/10.1016/0012-821X(83)90211-X

Watson, E., Wark D. A., & Thomas, J. (2006). Crystallization thermometers for zircon and rutile. *Contributions to Mineral and Petrology*, *151*, 413-433. https://doi.org/10.1007/s00410-006-0068-5

Wei, C., & Powell, R. (2004). Calculated phase relations in high pressure metapelites in the system NKFMASH (Na_2O-K_2O-FeO-MgO-Al_2O_3-SiO_2-H_2O). *Journal of Petrology*, *45*, 183-202. https://doi.org/10.1093/petrology/egg085

Wei, C., & Powell, R. (2006). Calculated phase relations in the system NCKFMASH (Na_2O-CaO-K_2O-FeO-MgO-Al_2O_3-SiO_2-H_2O) for high pressure metapelites. *Jounal of Petrology*, *47*, 385-408. https://doi.org/10.1093/petrology/egi079

Wendt, I., & Carl, C. (1991). The statistical distribution of the mean squared weighted deviation. *Chemical Geology Isotope Geoscience Section* 86, 275-285. http://dx.doi.org/10.1016/0168-9622(91)90010-T

Wolf, R., Farley, K., & Kass, D. (1998). Modeling of the temperature sensitivity of the apatite (U-Th)/He thermochronometer. *Chemical Geology*, *148*(1-2), 105-114. https://doi.org/10.1016/S0009-2541(98)00024-2

Wolf, R., Farley, K., & Silver, L. (1996). Helium diffusion and low-temperature thermochronometry of apatite. *Geochimica et Cosmochimica Acta*, *60*(21), 4231-4240. https://doi.org/10.1016/S0016-7037(96)00192-5

Wu, C.-M., Zhang, J. & Ren, L.-D. (2004a). Empirical Garnet-Biotite-Plagioclase-Quartz (GBPQ) Geobarometry in Medium- to High-Grade Metapelites. *Journal of Petrology*, *45*(9), 1907-1921. https://doi.org/10.1093/petrology/egh038

Wu, C.-M., Zhang, J., & Ren, L.-D. (2004b). Empirical garnet-muscovite-plagioclase-quartz geobarometry in medium- to high-grade metapelites. *Lithos*, *78*, 319-332. https://doi.org/10.1016/j.lithos.2004.06.008

Zeitler, P. (1985). Cooling history of the NW Himalaya, Pakistan. *Tectonics*, *4*(1), 127-151. https://doi.org/10.1029/TC004i001p00127

Zeitler, P., Johnson, N., Naeser, C., & Tahirkheli, R. (1982). Fission-track evidence for Quaternary uplift of the Nanga Parbat region, Pakistan. *Nature*, *298* (5871), 255-257. https://doi.org/10.1038/298255a0

Zen, E., & Hammarstrom, J. (1984). Magmatic epidote and its petrologic significance. *Geology*, *12*, 515-518. https://doi.org/10.1130/0091-7613(1984)12<515:MEAIPS>2.0.CO;2